

ESR detection of low-frequency fluctuations and optical-phonon-induced T_1 relaxation for $\text{KH}_2\text{PO}_4\text{:SeO}_4^{3-}$

B. Rakvin* and N. S. Dalal

Chemistry Department, West Virginia University, Morgantown, West Virginia 26506

(Received 25 July 1989)

Using the SeO_4^{3-} center as a paramagnetic probe, we have measured low-frequency (10^7 – 10^{10} -Hz) fluctuations in the paraelectric phase of KH_2PO_4 . The correlation time τ for these fluctuations, identified with the hopping of protons in $\text{O—H}\cdots\text{O}$ bonds, was found to exhibit an Arrhenius behavior, with an activation energy $\Delta E = 0.19 \pm 0.02$ eV and preexponential factor $\approx 1.0 \times 10^{-14}$ s. The non-Arrhenius behavior reported earlier for this system was ascribed to the omission of (a) inhomogeneous broadening due to proton spin-flip transitions and (b) a line-broadening process that depends exponentially on temperature. The latter process is suggested to be spin-lattice relaxation via optical phonons. The ΔE for this process was found to be essentially the same as that (≈ 0.19 eV) for the proton hopping, suggesting that the energy level of the optical phonon is located close to the top of the barrier. The phonon frequency is estimated to be 1500 ± 200 cm^{-1} for KH_2PO_4 and 1850 ± 200 cm^{-1} for KD_2PO_4 . These results are in partial agreement with some recent theoretical calculations and indicate new clues to the mechanism of the ferroelectric transition of these compounds.

I. INTRODUCTION

This paper reports on an ESR spin-probe study of some low-frequency ($\approx 10^7$ – 10^{10} Hz) molecular reorientations in KH_2PO_4 , henceforth abbreviated as KDP. The spin probe used was the SeO_4^{3-} center^{1–10} substituting sparsely for the PO_4^{3-} ions in the KDP lattice. The study was undertaken for the following reasons. First, recent experimental as well as theoretical investigations^{11–13} suggest that such low-frequency fluctuations are intrinsically related to the (still unclear) mechanism of the paraelectric-ferroelectric (or antiferroelectric) transitions of the KDP-type lattices, as well as of the proton-glass phenomenon exhibited by their mixed (ferroelectric + antiferroelectric) lattices. Second, the 10^7 – 10^{10} Hz frequency (ν) range falls naturally in the time scale of ESR spectroscopy, thus measurable conveniently by this technique. Third, while several earlier investigations^{1–3,7,10} have reported on ESR measurements of the correlation time, $\tau = 1/\nu$, for the KDP:SeO_4^{3-} system, there is some disagreement in the conclusions. For example, the temperature dependence of the τ has been interpreted as exhibiting an Arrhenius behavior [$\tau = \tau_0 \exp(\Delta E/kT)$] in some reports^{1,3,10} but a non-Arrhenius behavior in other studies.^{2,7} In addition, there is a large spread in the values reported for the activation energy, ΔE , ranging from 0.1 (Ref. 1) to 1 eV (Ref. 10), which is too large to be a result of measurement errors. Finally, we felt that the KDP:SeO_4^{3-} needed a reinvestigation in the light of our recent ESR investigations^{14,15} of the slow motion in other KDP-type lattices. These studies^{14,15} indicated that the non-Arrhenius behavior reported earlier for this system might be related to at least two line-broadening processes which were not recognized earlier: (a) a spin-lattice relaxation (T_1) process¹⁴ which leads to a broadening of the ESR signals, ex-

hibiting exponential dependence on temperature, and (b) an inhomogeneous broadening caused by the normally forbidden spin-flip ($\Delta M_s = \pm 1$, $\Delta M_l = \mp 1$) transitions.¹⁵ Our previous studies^{14,15} were, however, focused mainly on establishing the significance of these two mechanisms. We had thus investigated mainly the deuterated lattices (of the KDP family) because they provided high-resolution data (narrower ESR lines). In the present work we employ the previously described^{14,15} ESR linewidth analysis for KDP itself, which is the parent compound for this family of ferroelectrics and antiferroelectrics.¹⁶ We believe that the results obtained clarify the earlier controversies regarding the Arrhenius behavior and the magnitude of ΔE , and provide some new insight into the nature of the double-minimum potential well for the hydrogens in the $\text{O—H}\cdots\text{O}$ bonds. The ESR results on KDP are compared with the corresponding data on KD_2PO_4 (DKDP), available infrared and Raman scattering data,^{17,18} and theoretical predictions of Lawrence and Robertson¹⁹ on the vibronic levels of the $\text{O—H}\cdots\text{O}$ hydrogens in double-minimum potential wells.

II. EXPERIMENTAL

Single crystals of KDP doped with SeO_4^{2-} were grown from slowly cooling a saturated solution containing about 1 mol % K_2SeO_4 . The crystals grew as rectangular parallel pipes with the largest dimension as the c axis (the polar axis). The SeO_4^{3-} centers were formed via γ irradiation to a dose of ≈ 5 Mrad (not critical). All ESR measurements were made using a Bruker model ER 200D, X-band (9.5 GHz) spectrometer using 100 kHz magnetic-field modulation. The magnetic field was calibrated with a self-tracking NMR gaussmeter (Bruker, model ER 035M). The microwave frequency was measured with a Hewlett-Packard frequency counter, model 5340A. Tem-

perature variation was carried out using either a liquid nitrogen cryostat with a digital temperature controller (Bruker, model ER 4111 VT, accuracy ± 0.5 K) or an open-cycle helium cryostat with a digital temperature controller (Oxford Instruments, model ESR-900 with a DTC-2 controller, accuracy ± 0.1 K, stability ± 0.03 K).

III. EXPERIMENTAL RESULTS

Figure 1 shows a typical ESR spectrum of the SeO_4^{3-} center for the case of the crystal c axis oriented along the Zeeman field H . As described earlier,¹⁻⁵ the spectrum consists of a strong central line around 3340 G (at 9.3 GHz) originating from the $^{76,78,80}\text{Se}$ ($I=0$) isotopes and two weak satellites (at 2650 and 3880 G) from the large (≈ 1200 G) hyperfine interaction of the ^{77}Se ($I=\frac{1}{2}$, 9.6% abundant) nucleus. The line at 2650 G is the so-called¹⁻¹⁰ low-field (LF), and the 3880-G signal is the high-field (HF) hyperfine component. The 1:4:6:4:1 quintet structure on each signal arises from the superhyperfine coupling of four "dynamically equivalent" protons, as explained earlier.¹⁻⁵

In this work we focus on the LF and HF lines because the central (3340 G) portion is overlapped by signals from other radicals. From a comparison of the shapes of the LF and HF signals at 180 and 280 K (Fig. 1) it can be verified that the linewidths increase with increase in temperature, so much so that the proton superhyperfine structure is not resolved above 280 K. Figure 2 shows the temperature dependence of the peak-to-peak linewidth, Γ , for this orientation ($H\parallel c$). In the range from 285 to 335 K the signal is a single, broad component, with its Γ increasing rapidly with temperature, as reported earlier¹⁴ for $\text{DKDP}:\text{SeO}_4^{3-}$. Below 240 K, however, for KDP the line broadening becomes small enough so that the underlying proton superhyperfine structure becomes evident. Thus, below 240 K, Γ was measured as the peak-to-peak width of the outer component of superhyperfine quintets. The outer components were selected because they are not much affected by proton exchange.² These data are indicated via the solid squares

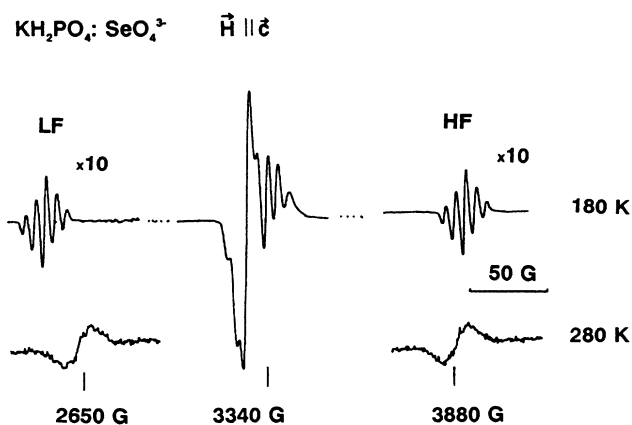


FIG. 1. Typical ESR spectra of $\text{KH}_2\text{PO}_4:\text{SeO}_4^{3-}$ for $H\parallel c$. Notice the increased linewidths of the higher temperature (280 K) spectra.

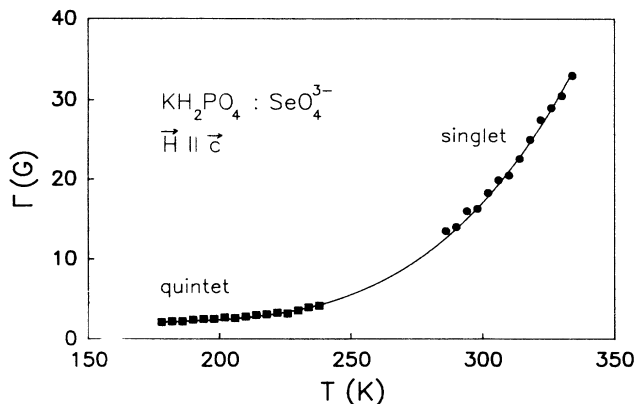


FIG. 2. Temperature dependence of the peak-to-peak linewidth (Γ) of the ESR spectra for $\text{KH}_2\text{PO}_4:\text{SeO}_4^{3-}$, for $H\parallel c$. Solid squares (\blacksquare) correspond to the width of a single component of the proton superhyperfine quintet, and solid circles (\bullet) to that of the whole signal because in this temperature range the overall broadening is much larger than the superhyperfine coupling.

(\blacksquare) in Fig. 2. It will be shown below that the mechanism causing the broadening is the same for the entire temperature range, whether measured from a single superhyperfine component or from the entire signal (where the superhyperfine structure is not resolved).

Figure 3 shows the temperature dependence of some typical spectra for $H\parallel a$ where the main (doublet) splitting originates from two differently oriented molecular sites in

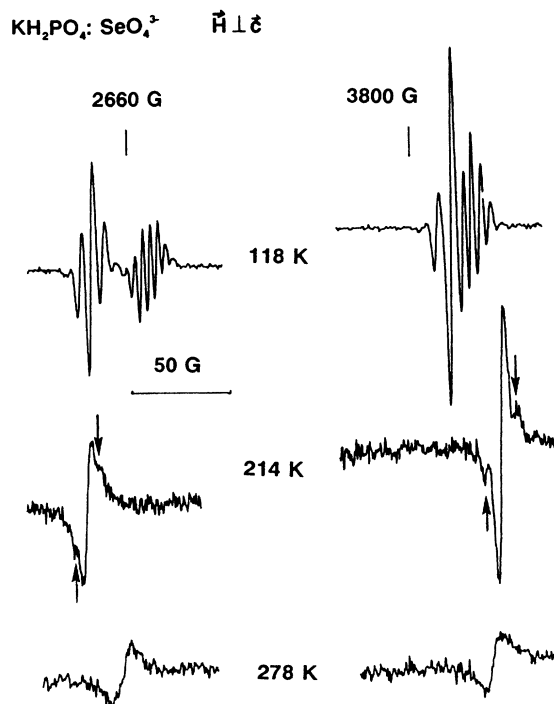


FIG. 3. Typical ESR spectra of $\text{KH}_2\text{PO}_4:\text{SeO}_4^{3-}$ for $H\parallel a$, exhibiting motional narrowing (214 K) and a rapid broadening with further increase in temperature (278 K). The arrows highlight the positions of the proton spin-flip transitions discussed in the text.

a given domain.⁵ For this orientation there are two separate temperature regimes characterized by a temperature T^* , the coalescence temperature for the domain splitting, as discussed in numerous earlier publications.^{1-10,14,15} The sharp, multiline, structure on each component arises from the proton superhyperfine structure, as discussed for $\mathbf{H}\parallel c$ (Fig. 1). As the sample temperature T is raised to T^* , each of the doublet components broadens, and finally, at $T = T^*$ they coalesce into a singlet. Note, however, that the T^* values for the HF and the LF lines are 158 and 170 K respectively because of their different doublet splittings (Fig. 4). As the temperature is raised above T^* , the coalesced singlet keeps on narrowing for about 20 K, as expected for the narrowing in the limit of fast motion.⁵ This may be noted from the spectra at 214 K. On further temperature increase, however, the signals start to broaden rapidly, as may be verified from the spectra at 278 K (Fig. 3, bottom). The temperature dependence of the measured peak-to-peak linewidths is shown in Fig. 4. Here the triangles denote the linewidth data below T^* for the LF component, while the circles and the squares correspond to the widths for the LF and HF lines for $T > T^*$. We note that in Fig. 4 the linewidth data for the ± 20 K range around T^* (≈ 170 K) are qualitatively similar to the measurements reported earlier.¹⁻⁵ However, a new feature was the detection of the rapid increase above 300 K for both the LF and the HF line. While the presently observed broadening of both of the lines (for KDP) is in a qualitative agreement with our earlier results¹⁴ for KD_2PO_4 (DKDP), it disagrees with a recent study¹⁰ on KDP wherein it was reported that only one of the lines (the HF line) shows the broadening. The cause of this discrepancy is not understood.

Another new observation was the detection of proton spin-flip ($\Delta M_s = \pm 1, \Delta M_I = \mp 1$) transitions for both the HF and the LF lines, as highlighted by the arrows in Fig. 3. While the possibility of such transitions had been suspected earlier^{2,3} the present work provides clear proof

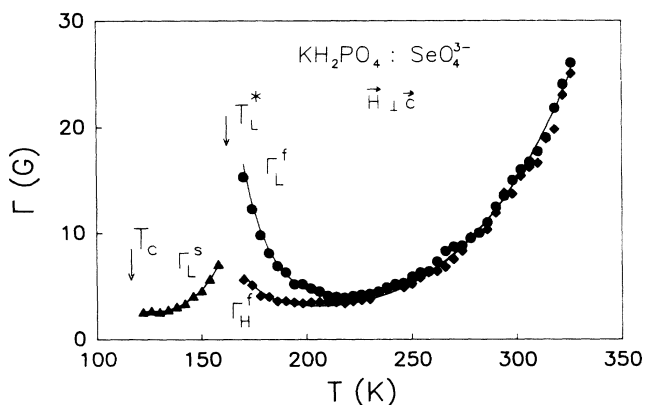


FIG. 4. Temperature dependence of the peak-to-peak linewidth for $\text{KH}_2\text{PO}_4:\text{SeO}_4^{3-}$, $\mathbf{H}\parallel c$. T^* is the coalescence temperature for the low-field (LF) ^{77}Se hyperfine component. The subscripts L and H correspond to the LF or the HF hyperfine component, while the superscripts s and f signify the “slow” or the “fast” motion regimes respectively.

of these transitions: Their separation equals $2g_n\beta_nH$ (for protons), their intensity increases with increase in microwave power, and their intensity decreases rapidly on deuteration. As discussed earlier¹⁵ for the AsO_4^{4-} center in KH_2AsO_4 and KD_2AsO_4 , these lines do make a significant contribution to the overall linewidth and were included in the linewidth analysis.

IV. LINEWIDTH ANALYSIS

We noted that the temperature dependence of the linewidth for $\text{KDP}:\text{SeO}_4^{3-}$ (Figs. 2 and 4) was qualitatively similar to that reported recently^{14,15} for the CrO_4^{3-} , SeO_4^{3-} , and AsO_4^{4-} probes in DKDP. Since the analysis procedure used for DKDP had provided a satisfactory description of the experimental observations, the same procedure was used for KDP. This procedure has been outlined in detail earlier,^{14,15} thus, only the necessary details will be given here.

A. Slow-motion regime ($T < T^*$)

As follows from standard theories of motional narrowing, such as the modified Bloch equations,²⁰ on approaching the coalescence temperature T^* (from $T < T^*$) each component of a doublet related by motional exchange exhibits a linewidth increase. On the basis of the modified Bloch equations in the “slow motion” regime, this linewidth increase is given by²⁰

$$\Gamma^s = \Gamma_0 + c/2\gamma\tau, \quad T < T^*, \quad (1)$$

where Γ^s is the peak-to-peak linewidth, s signifying the slow motion regime.²⁰ Γ_0 is the residual linewidth at low ($T \ll T^*$) temperature, γ is the gyromagnetic ratio, and c is a constant whose value depends on the lineshape: 1.15 for a Lorentzian and 1.7 for a Gaussian lineshape.

Assuming that the motional process represented by τ is thermally activated [i.e., $\tau = \tau_0 \exp(\Delta E/kT)$], Eq. (1) can be written as

$$\Gamma^s = \Gamma_0 + (c/2\gamma\tau_0)e^{-\Delta E/kT} \quad (2)$$

and

$$\ln(\Gamma^s - \Gamma_0) = \ln(c/2\gamma\tau_0) - \Delta E/kT. \quad (3)$$

Thus, if τ followed an Arrhenius behavior then a plot of $\ln(\Gamma^s - \Gamma_0)$ versus T^{-1} should be linear with a slope proportional to ΔE . This was indeed found to be the case as may be noted from Fig. 5 where the solid circles (\bullet) are the measured data points and the solid line is the fitted curve. The activation energy (ΔE) obtained was ≈ 0.19 eV, in a reasonable agreement with some of the earlier reports.^{2,5}

B. Fast motion: motional narrowing regime ($T \geq T^*$)

As discussed earlier^{14,15} in the “fast” motion regime the linewidths can be described by the following result of the modified Bloch equations²⁰

$$\Gamma^f = \Gamma_0 + c\gamma\delta_0^2\tau/4 \quad (4)$$

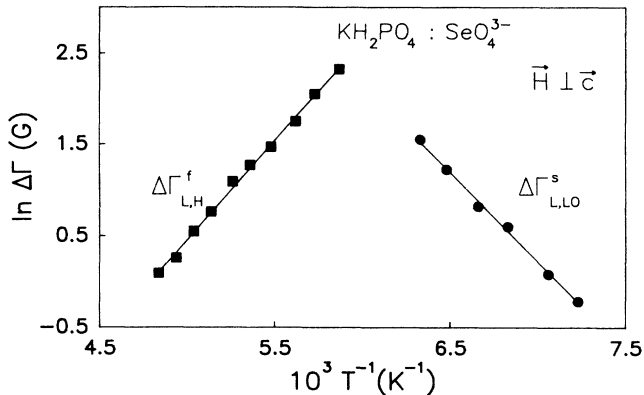


FIG. 5. A logarithmic plot of the peak-to-peak linewidth differences ($\Gamma_h^f - \Gamma_l^f$) and ($\Gamma_h^s - \Gamma_l^s$) vs inverse temperature for the data in Fig. 4.

where “*f*” signifies the “fast” motion regime, and δ_0 is the splitting in the limit of motional freezing, the so-called residual splitting.

As before, it was useful to note that the LF and the HF lines exhibit slightly different doublet splittings, δ_0 (≈ 26 G for the LF, and ≈ 9 G for the HF line). Thus, the unknown, residual broadening, Γ_0 , in Eq. (4) could be largely eliminated by employing the differences ($\Delta\Gamma$) in the widths of these two lines. Using Eq. (4), one obtains $\Delta\Gamma$ as

$$\Delta\Gamma = \Gamma_l - \Gamma_h = \Gamma_{0l} - \Gamma_{0h} + c\gamma\tau(\delta_{0l}^2 - \delta_{0h}^2)/4, \quad (5)$$

with

$$(\Gamma_{0l} - \Gamma_{0h}) \ll c\gamma\tau(\delta_{0l}^2 - \delta_{0h}^2)/4. \quad (6)$$

Here the subscripts *l* and *h* signify the “low” and the “high” field hyperfine components, and Γ_{0l} and Γ_{0h} are their low temperature, residual linewidths. We noted that since Eq. (5) contains τ , it permits a simple procedure for examining the probe’s Arrhenius behavior, by writing it as

$$\Delta\Gamma = (\Gamma_{0l} - \Gamma_{0h}) + \frac{1}{4}c\gamma\tau_0(\delta_{0l}^2 - \delta_{0h}^2)e^{\Delta E/kT}. \quad (7)$$

Thus, a plot of $\ln\Delta\Gamma$ versus T^{-1} should be linear if τ obeyed the Arrhenius equation. Using the measured values for Γ_l and Γ_h (Fig. 4), we plotted $\ln\Delta\Gamma$ as a func-

tion of T^{-1} , as shown in Fig. 5. It is seen that the plot is linear over a wide temperature range. The slope of this line yields an activation energy of $\approx 0.19 \pm 0.02$ eV. It is worth stressing that this value is essentially the same as found from the slow motion proton fluctuation data (previous section).

An important precautionary note is that in this temperature range the spin-flip transitions make significant contribution to the peak-to-peak linewidths. This is because their separation ($2g_n\beta_n H$) becomes equal to the peak-to-peak linewidths (cf. Fig. 3). Moreover the temperature at which this happens is different for the LF and the HF lines. It is helpful to note that since the separations of the spin-flip transitions are temperature independent, while the motional broadening is strongly temperature dependent, a systematic temperature dependence study can help isolate the inhomogeneous broadening due to the spin-flip transitions.¹⁵

As discussed earlier,^{14,15} the procedure of taking the linewidth differences becomes inaccurate when $\Gamma_l \approx \Gamma_h$. This is the case for the data at temperature above 215–220 K, as may be noted from Fig. 4. Moreover, above this temperature both of the lines start to exhibit rapid broadening, which can be explained in terms of a spin-lattice relaxation (T_1) broadening, as discussed below.

C. Fast motion: Linewidth increase, $T \gg T^*$ regime

In the temperature regime above 220 K, the linewidth increases rapidly, for both $\mathbf{H}||c$ (Fig. 2) and $\mathbf{H}\perp c$ (Fig. 4). Based on the procedure discussed earlier,^{14,15} the linewidth data in the whole fast motion regime (220–340 K) were fitted to the following equation:¹⁴

$$\Gamma = \Gamma_0 + Ae^{\Delta E/kT} + Be^{-\Delta E/kT}. \quad (8)$$

The continuous lines in Figs. 2 and 4 represent the fits to Eq. (8), with the parameters listed in Table I.

D. Calculation of τ

The correlation time τ was also calculated via essentially the same procedure as discussed earlier.^{14,15} Briefly, since the activation energy ΔE was found to be the same ($\approx 0.19 \pm 0.02$ eV) for the slow and the fast motion regimes, for $\mathbf{H}||c$ as well as $\mathbf{H}\perp c$, this value was considered

TABLE I. Parameters describing ESR linewidths for the SeO_4^{3-} center in KDP and DKDP. LF indicates the low-field (≈ 2600 G) line; HF, the high-field (≈ 3800 G) line.

Lattice/Orientation			<i>A</i> (G)	<i>B</i> (G)	Γ_0 (G)	τ_0 (s)	ΔE (eV) ^a
KDP	$\mathbf{H} c$	HF		2.0×10^4	2.0	1×10^{-14}	0.19
KDP	$\mathbf{H}\perp c^b$	LF	3.4×10^{-5}	1.9×10^4	2.3	1×10^{-14}	0.19
KDP	$\mathbf{H}\perp c^b$	HF	0.4×10^{-5}	1.9×10^4	2.3	1×10^{-14}	0.19
DKDP ^c	$\mathbf{H}\perp c^d$	LF	1.8×10^{-5}	3.2×10^4	4.1	6×10^{-15}	0.22
DKDP ^c	$\mathbf{H}\perp c^d$	HF	0.2×10^{-5}	3.2×10^4	4.1	6×10^{-15}	0.22

^aThe error in ΔE is estimated to be ± 0.02 eV, corresponding to the accuracy of measurement of Γ_0 of ± 0.3 G.

^b $\mathbf{H}||a$.

^cData from Ref. 14. In Table I of Ref. 14 constant *B* should read 3.2×10^3 instead of 3.2×10^4 .

^d $\mathbf{H}||(\mathbf{a} + 45^\circ)$.

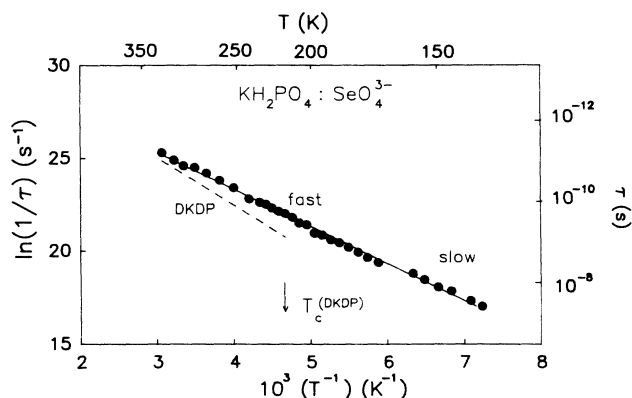


FIG. 6. An Arrhenius plot of the correlation time τ for $\text{KH}_2\text{PO}_4:\text{SeO}_4^{3-}$ for both the "fast" and the "slow" motion regimes, as indicated. The dashed line represents the data for $\text{KD}_2\text{PO}_4:\text{SeO}_4^{3-}$ taken from Ref. 14.

to be fairly representative. We thus needed to evaluate only τ_0 critically. Because $\tau = \tau_0 \exp(\Delta E/kT)$, an uncertainty of 10% in ΔE (as is the case here) translates into an order of magnitude error in τ_0 . Moreover, there are several independent procedures for deducing τ_0 (i.e., slow motion regime, coalescence point, etc.). Based on our earlier experience^{14,15} with several probes and lattices, we find that the procedure based on parameter A yields an accurate value for τ_0 , because this parameter is derived from a large number of experimental observations. This procedure yielded $\tau_0 \approx 1 \times 10^{-14}$ s for KDP, as compared to 6×10^{-15} s for DKDP.¹⁴

Figure 6 shows the temperature dependence of τ for the whole temperature range, as deduced from the data for the LF line. The fast and the slow motion regimes are indicated in Fig. 6. It is seen that the linewidth data for the whole temperature (130–340 K) range can be described by the Arrhenius equation with $\Delta E = 0.19 \pm 0.02$ eV, and $\tau_0 = 1 \times 10^{-14}$ s. These values are included in Table I, which also contains the corresponding data for DKDP from Ref. 14. The dashed line in Fig. 6 represents the data for DKDP (taken from Ref. 14), exhibiting an isotope effect on the τ values.

V. DISCUSSION

A. Arrhenius behavior and activation energy

The linearity of the plot in Fig. 6 clearly shows that for $\text{KDP}:\text{SeO}_4^{3-}$ the τ exhibits an Arrhenius behavior over 130–340 K. Thus, the earlier observed non-Arrhenius behavior² can be ascribed to the omission of at least two processes: (a) the high-temperature broadening effect, and (b) the inhomogeneous broadening caused the spin-flip transitions. We also noted that for KDP the activation energy of 0.19 eV is the same as that reported by Hukuda² for the restricted region (140–180 K) where an Arrhenius behavior was noted, but differs from the value of 1.07 ± 0.05 eV reported recently by Owens¹⁰ for the 310–360 K range. The results on KDP are in accord with an earlier study on DKDP.¹⁴

B. Interpretation of ΔE

The present study on KDP and earlier investigations^{14,15} of related compounds (KD_2PO_4 , KD_2AsO_4 , $\text{NH}_4\text{H}_2\text{AsO}_4$, $\text{ND}_4\text{D}_2\text{AsO}_4$, and $\text{ND}_4\text{D}_2\text{PO}_4$) establish that the activation energy ΔE for the high-temperature ($T \gg T^*$) broadening process is essentially the same as that for the proton hopping around T^* . A clue to the origin of ΔE was obtained from the fact that the high-temperature broadening exhibits an exponential dependence on temperature. Earlier theoretical studies by Huang²¹ and by Kumar and Sinha²² have shown that the spin-lattice relaxation time (T_1) of paramagnetic centers caused by two-phonon Raman processes, involving optical phonons, depends exponentially on temperature. This is similar to the two-phonon Orbach relaxation process involving acoustical phonons. This type of exponential temperature dependence of ESR linewidths has been observed for the Cr^{3+} and Fe^{3+} paramagnetic ions in MgO crystals,^{23,24} and ascribed to a T_1 process governed by optical phonons.^{23,24} Some earlier evidence that optical phonons play an important role in the spin-lattice relaxation mechanism for KH_2AsO_4 (KDA) at temperature around T_c has been reported by Weisensee *et al.*,²⁵ for $\text{KDP}:\text{SeO}_4^{3-}$ by Wheeler *et al.*^{8,9} and for other hydrogen-bonded ferroelectrics by Volkel *et al.*²⁶ However, all of these studies were carried out at much lower temperatures than T^* . The frequency of the optical phonons involved in the relaxation process in this temperature range was of the order of 100 cm^{-1} . If the same mechanism holds at $T \gg T^*$, in the present case, then the frequency of the relevant optical phonons would be $\approx \Delta E/h = 1500 \text{ cm}^{-1}$ for KDP and 1800 cm^{-1} for DKDP. These phonons should be detectable via Raman and/or infrared measurements. Data in the literature^{17,18} show that the vibrational spectra of the KDP-type of crystals in this (high) frequency region arise from vibrations involving mainly the $\text{O}-\text{H} \cdots \text{O}$ or $\text{O}-\text{D} \cdots \text{O}$ bonds. In particular, Raman scattering data¹⁸ for both KDP and DKDP do show a strong band 1790 cm^{-1} , with a width of about 250 cm^{-1} . In addition DKDP exhibits a strong band at 1990 cm^{-1} while KDP exhibits bands at 2360 and 2700 cm^{-1} . Thus, for the temperature range investigated in present the work (300–350 K) the band closest to our ΔE value is the band around 1800 cm^{-1} providing some support for the interpretation that ΔE corresponds to the difference in the energy of the ground state and the excited state that is closest to the top of the barrier.

Since the observed ΔE seems to be related mainly to the vibration of the $\text{O}-\text{H} \cdots \text{O}$ bonds, ΔE should also be compared to the recent theoretical calculations of Lawrence and Robertson.¹⁹ These authors have proposed a (double) Morse potential model of the double-minimum potential for the $\text{O}-\text{H} \cdots \text{O}$ bonds in KDP, and for the $\text{O}-\text{D} \cdots \text{O}$ bonds in DKDP. In this model the process causing polarization fluctuations can be identified with the transfer of protons from one side of the well to another. The activation energy for the process should be the difference in the energy of the ground state and the excited state that is located closest to the

top of the barrier. For DKDP they have assigned this energy to 1750 cm^{-1} in excellent (perhaps fortuitous) agreement with our reported ΔE value of $0.22 \pm 0.02 \text{ eV} \equiv 1775 \pm 160 \text{ cm}^{-1}$. For KDP, the presently reported¹⁴ value of $0.19 \pm 0.02 \text{ eV} \equiv 1532 \pm 160 \text{ cm}^{-1}$ is in disagreement with their value of 2130 cm^{-1} . Lawrence and Robertson note, however, that their calculation¹⁹ does not directly involve the energy of the level closest to the barrier, hence there could be a considerable uncertainty in the corresponding position. We thus believe that our results are not necessarily in disagreement with their calculation.

VI. CONCLUSIONS

The present work shows that in both KDP and DKDP, there exist low-frequency ($10^7 - 10^{10} \text{ Hz}$) fluctuations of the hydrogen bonded protons (or deuterons). The underlying motions appear to be related to (slow) fluctuations of polarization "clouds" near the paramag-

netic center. Such fluctuations appear to be a common phenomenon for all KDP-type ferroelectrics, regardless of the paramagnetic probe. The correlation time, τ , for these fluctuations exhibits Arrhenius behavior, with activation energy $0.19 \pm 0.02 \text{ eV}$ for KDP. This agrees with the earlier reported¹⁴ value of $0.22 \pm 0.02 \text{ eV}$ for DKDP. Because the activation energy for the polarization fluctuations (which involve barrier crossing) is essentially the same as that for the T_1 process (which need not involve barrier crossing), classically, ΔE may be identified with the barrier height. An alternate interpretation is that the phonon level involved in the T_1 process is located close to the top of the energy barrier. The energy-level separation deduced, for DKDP, from ESR, agree very well with a recent theoretical model¹⁹ of the motion of the hydrogens in the double-minimum potential wells of the KDP-type compounds. The methodology presented here appears to provide an easy way of investigating the nature of the energy levels involved in such interactions, as a complement to other spectroscopic techniques.

*Permanent address: Ruder Boskovic Institute, University of Zagreb, P.O. Box 1016, 41001 Zagreb, Croatia, Yugoslavia.

¹T. Kawano, J. Phys. Soc. Jpn. **37**, 848 (1974).

²K. Hukuda, J. Phys. Soc. Jpn. **38**, 150 (1975).

³N. S. Dalal, J. A. Hebden, D. E. Kennedy, and C. A. McDowell, J. Chem. Phys. **66**, 4425 (1977).

⁴N. S. Dalal, J. Am. Chem. Soc. **104**, 5512 (1982).

⁵For a review, see, N. S. Dalal, Adv. Magn. Reson. **10**, 119 (1982).

⁶N. S. Dalal, Ferroelectrics **49**, 93 (1983).

⁷Y. Matsumoto, S. Akahoshi, and K. Hukuda, J. Phys. Soc. Jpn. **53**, 3046 (1984).

⁸D. D. Wheeler, H. A. Farach, and C. P. Poole, Jr., Phys. Lett. **103B**, 144 (1984).

⁹D. D. Wheeler, H. A. Farach, C. P. Poole, Jr., and R. J. Creswick, Phys. Rev. B **37**, 9703 (1988).

¹⁰F. J. Owens, J. Chem. Phys. **87**, 6066 (1987).

¹¹See, for example, R. Blinc and B. Zeks, Ferroelectrics **72**, 193 (1987); V. H. Schmidt, *ibid.* **72**, 157 (1987); **78**, 207 (1988) and references therein.

¹²E. Courtens, J. Phys. Lett. **43**, L-199 (1982); Phys. Rev. Lett. **52**, 69 (1985); Jpn. J. Appl. Phys. **24**, Suppl. 2, 70 (1985).

¹³E. Courtens and R. Vacher, Phys. Rev. B **35**, 7271 (1987); V. Dobrosaljevic and R. Stratt, Phys. Rev. B **36**, 8484 (1987).

¹⁴N. S. Dalal and B. Rakvin, J. Chem. Phys. **90**, 5262 (1989).

¹⁵B. Rakvin and N. S. Dalal, Phys. Rev. B **39**, 7009 (1989).

¹⁶M. E. Lines and A. M. Glass, *Principles and Applications of Ferroelectrics and Related Materials*, (Clarendon, Oxford, 1977), Chap. 9.

¹⁷R. P. Lowndes, N. E. Tornberg, and R. C. Leung, Phys. Rev. B **10**, 991 (1974).

¹⁸I. P. Kaminow, R. C. C. Leite, and S. P. S. Porto, J. Phys. Chem. Solids **26**, 2085 (1965).

¹⁹M. C. Lawrence and G. N. Robertson, Ferroelectrics **25**, 363 (1980); M. C. Lawrence and G. N. Robertson, J. Phys. C **13**, L1053 (1980).

²⁰See, for example, J. E. Wertz and J. R. Bolton, *Electron Spin Resonance—Elementary Theory and Practical Applications* (McGraw-Hill, New York, 1972), Chap. 9.

²¹C. Y. Huang, Phys. Rev. **154**, 215 (1967).

²²N. Kumar and K. P. Sinha, Physica **34**, 387 (1967).

²³G. F. Imbusch, W. M. Yen, A. L. Schawlow, and D. E. McCumber, Phys. Rev. A **133**, 1029 (1964).

²⁴R. L. Hartman, A. C. Daniel, J. S. Bennett, and J. G. Castle, Bull. Am. Phys. Soc. **11**, 313 (1966).

²⁵U. Weisensee, G. Volkel, and W. Brunner, Solid State Commun. **48**, 309 (1983).

²⁶G. Volkel, W. Brunner, and H. E. Muller, Ferroelectrics **78**, 267 (1988).